

Simplifications in the x-ray line-shape analysis

T. Adler and C. R. Houska

Citation: *Journal of Applied Physics* **50**, 3282 (1979); doi: 10.1063/1.326368

View online: <http://dx.doi.org/10.1063/1.326368>

View Table of Contents: <http://scitation.aip.org/content/aip/journal/jap/50/5?ver=pdfcov>

Published by the [AIP Publishing](#)

Articles you may be interested in

[Importance of line shape calculations in x-ray laser modelling](#)

AIP Conf. Proc. **645**, 445 (2002); 10.1063/1.1525486

[X-ray photoemission of carbon: Lineshape analysis and application to studies of coals](#)

J. Appl. Phys. **53**, 6857 (1982); 10.1063/1.330025

[Least-squares analysis of x-ray diffraction line shapes with analytic functions](#)

J. Appl. Phys. **52**, 748 (1981); 10.1063/1.328757

[Automatized X-Ray Line Profile Analysis](#)

Rev. Sci. Instrum. **34**, 684 (1963); 10.1063/1.1718540

[Simplifications in X-Ray Diffraction Line Breadth Analysis](#)

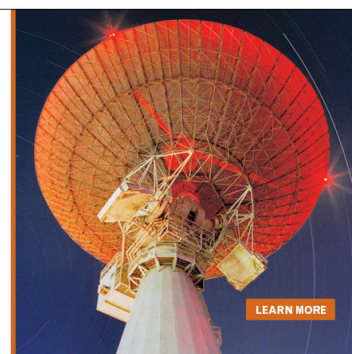
J. Appl. Phys. **30**, 2016 (1959); 10.1063/1.1735111

MIT LINCOLN
LABORATORY
CAREERS

Discover the satisfaction of
innovation and service
to the nation

- Space Control
- Air & Missile Defense
- Communications Systems & Cyber Security
- Intelligence, Surveillance and Reconnaissance Systems
- Advanced Electronics
- Tactical Systems
- Homeland Protection
- Air Traffic Control

 **LINCOLN LABORATORY**
MASSACHUSETTS INSTITUTE OF TECHNOLOGY



Simplifications in the x-ray line-shape analysis

T. Adler and C. R. Houska

Department of Materials Engineering, Virginia Polytechnic Institute and State University, Blacksburg, Virginia 24061

(Received 9 October 1978; accepted for publication 5 December 1978)

It is shown that a Fourier series associated with the Warren-Averbach line-shape analysis can be fitted with only five parameters to a pair of peaks. These interrelate the Fourier coefficients and thereby provide a simplified series which has been applied to the study of a Mo film on a Si crystal. The parameters include the average particle size, the first neighbor rms strain, a term which gives the variation in rms strain with cell separation, and two instrumental broadening coefficients. Although considerable simplification is possible, equivalent information can be obtained as compared with the original analysis and the "hook effect" is eliminated in the fitted coefficients.

PACS numbers: 61.70. - r, 61.80.Cb

INTRODUCTION

The interpretation of x-ray line profiles from either films deposited onto substrates or films reacted with their substrate presents special difficulties that are not usually present in homogeneous single-phase materials. If accurate line profiles are obtainable, which can be separated from adjacent peaks, the Warren-Averbach analysis¹ offers a powerful approach in determining the residual nonuniform strain and particle-size contributions to the broadening. Very few assumptions are required with this approach. Unfortunately, in film studies, overlapping profiles are the rule rather than the exception. Therefore, it is not certain whether meaningful results can be obtained using an elaborate line-shape analysis. For example, a profile which requires 20–50 Fourier coefficients contains the same number of adjustable parameters. Errors in the profile could generate considerable error in these coefficients especially those associated with the slowly varying tail portion of a peak. Sufficient data are now available to reveal that the number of required parameters can be reduced to as few as five for a pair of peaks. This is possible because simple relationships can be found between the particle size and strain coefficients within the Fourier series representation of the profile. Analytical forms are available from quantitative microscopy that allow the particle-size coefficient to be further simplified, while accurate rms strain data follow a simple functional dependence with the separation between cells when corrected for the "hook effect." Although considerable simplification is possible, information equivalent to the original analysis can still be obtained. These simplifications are discussed and an example is given for Mo deposited onto a Si crystal. The authors believe that this simplified Fourier approach will be of considerable value in studies where overlapping line profiles occur. The affect of stacking faults usually modifies the particle-size term. This has been treated elsewhere^{2,3} and need not be repeated here.

THEORY

Nonuniform strain

The line shape for a polycrystalline material containing

both strains and small particle size is given by the Fourier series¹

$$P'(\theta) = \frac{KNF^2}{\sin^2\theta} \sum_n A_n \cos[2\pi n(h_3 - l)], \quad (1)$$

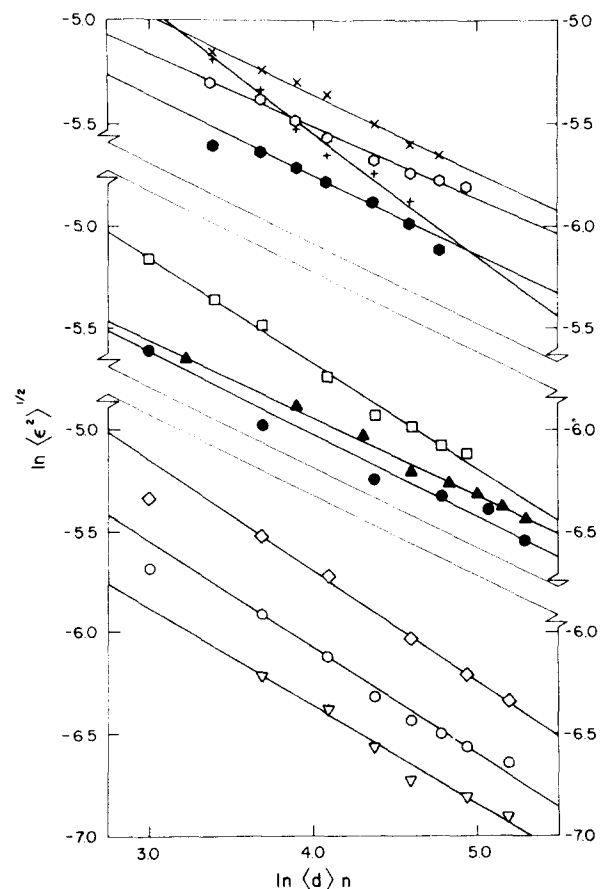


FIG. 1. Examples of the validity of $\langle \epsilon_n^2 \rangle^{1/2} = |n| \langle \epsilon_n^2 \rangle^{1/2}$ where $\ln \langle \epsilon_n^2 \rangle^{1/2}$ and $r \ln \langle d \rangle |n|$ are taken from data having a minimum influence of overlapping lines. That is, the stronger 110 and 220 were used for bcc, the 111 and 222 for fcc, while all measurable reflections were used for isotropic W. \times —niobium (110); $+$ —tantalum (110); \circ —vanadium (110); \circ —chromium (110); \bullet —shot peened 1018 steel (110); \square — α -brass filings (111); \blacktriangle —thoriated tungsten filings; \diamond —cold-worked Mo (110); \circ —Mo (110) annealed at 415 °C; ∇ —Mo (110) annealed at 660 °C.

TABLE I. Values of r and $\langle \epsilon_1^2 \rangle^{1/2}$ for various materials and crystal directions.

Material	Ref.	hkl	$\langle d \rangle$	r	$\langle \epsilon_1^2 \rangle^{1/2}$
Thoriated tungsten (filings)	1	110	2.238	-0.380	0.00885
1018 steel (shot peened)	9	110	2.027	-0.460	0.00937
Molybdenum (filings)	7	110	2.225	-0.559	0.0201
Molybdenum (filings) annealed at 415 °C	7	110	2.225	-0.524	0.0123
Molybdenum (filings) annealed at 660 °C	7	110	2.225	-0.481	0.00803
α -brass (65-35) (filings)	6	111	2.130	-0.515	0.01819
α -brass (65-35) (filings annealed at 225 °C)	6	111	2.130	-0.508	0.01165
Niobium (filings)	8	110	2.334	-0.376	0.0155
Vanadium (filings)	8	110	2.149	-0.325	0.0119
Chromium (filings)	8	110	2.040	-0.360	0.0107
Tantalum (filings)	8	110	2.335	-0.606	0.0264
				Average: -0.463	

where h_3 is a variable in reciprocal space given by $h_3 = 2\langle d \rangle \sin\theta / \lambda$, $\langle d \rangle$ is the average interplanar spacing for the (001) planes, θ is the angle of incidence, and λ the wavelength. Other terms in Eq. (1) include a constant K , N is the number of diffracting cells, and F is the structure factor. The coefficients are given as a product of a particle size term, A_n^S , and a distortion coefficient which is given by

$$A_n^D = \exp(-2\pi^2 \langle \epsilon_n^2 \rangle n^2 l^2). \quad (2)$$

Nonuniform strain is contained in Eq. (2), while a uniform strain may be identified by comparing $\langle d \rangle$ with the corresponding value from a standard which is strain free. This is determined simply from the relative peak shift as in a residual stress analysis.⁴ Most often the peak profile is symmetrical after a correction is made for instrumental broadening and only a cosine series is required. A discussion of the instrumental broadening is given later.

The $\ln \langle \epsilon_L^2 \rangle$ versus $\ln n$ was plotted in order to simplify the analysis from one containing a large number of apparently unrelated experimental Fourier coefficients⁵⁻⁹ to only a few parameters. In each case, the plot was a straight line with no systematic departures (see Fig. 1). When departures are apparent, the Fourier coefficients contained a hook effect at small n due to the difficulty in allowing for slowly varying background. The linearity of a ln-ln plot suggests that all data follow the simple relation

$$\langle \epsilon_n^2 \rangle^{1/2} = |n|^r \langle \epsilon_1^2 \rangle^{1/2}. \quad (3)$$

For cold-worked samples r ranges from -0.38 to -0.61 (see Table I) which appears to be a surprisingly restricted spread about an average value of -0.46. A value of $-\frac{1}{2}$ was previously reported in an earlier work by Rothman and Cohen using fewer data points.³ The Appendix includes a development by Mering¹⁰ which is not well known. In this case, a value of $-\frac{1}{2}$ is also obtained which does not depend on the strain distribution provided they are independent for successive cells in a column. The parameters r and $\langle \epsilon_1^2 \rangle^{1/2}$ can be of

considerable interest in relating the line-shape results to the distribution of defects.

In developing Eq. (1), the product $\langle d \rangle Z_n$ is used to describe the displacement of cells separated by a distance $\langle d \rangle n$. Both distances are along a direction perpendicular to the diffracting planes. The quantity Z_n is in units of $\langle d \rangle$ and is related to strain by $\epsilon_n = Z_n/n$. For $n = 1$, $\epsilon_1 = Z_1$. Rewriting Eq. (3) on this basis and squaring gives

$$\langle Z_n^2 \rangle = |n|^{2(r+1)} \langle Z_1^2 \rangle. \quad (4)$$

It would be appropriate to comment on the exponential form of Eq. (2) since this may be obtained in two ways. As the exponent becomes small, this approximation becomes more exact irregardless of the distribution. The form is rigorous when the strain ϵ_n or displacements Z_n are given by a Gaussian distribution at each value of n . The fact that this exponent is very often greater than unity for $l = 2$ and that $\ln A_n^D$ versus l^2 is linear except for the largest values of n and l would indicate that the strain closely follows a Gaussian distribution. When the data are sufficiently complete and accurate the distribution can be shown to be closely Gaussian.^{5,11,12} Equations (3) and (4) provide a relationship for the variation in variance with distance if the Gaussian form is adopted, i.e.,

$$P(Z_n) = \frac{1}{(2\pi \langle Z_n^2 \rangle)^{1/2}} \exp\left[-\frac{1}{2} \left(\frac{Z_n}{\langle Z_n^2 \rangle^{1/2}}\right)^2\right]. \quad (5)$$

There has been no evidence in support of another distribution for cold-worked metals. However, evidence does exist that the distribution is closely Gaussian even for neutron-irradiated materials.

One can attain various limiting profile shapes by the proper selection of r . These are listed in Table II. If $r = 1$, all relative displacements $\langle Z_n^2 \rangle$ are equal to $\langle Z_1^2 \rangle$ allowing a common term to be factored from the Fourier series. This behaves like a temperature term by scaling the sum of a series containing only particle-size coefficients. The sum with only

TABLE II. Relationships between nonuniform strain, displacement, strain Fourier coefficient, and r .

r	$\langle \epsilon_n^2 \rangle$	$\langle Z_n^2 \rangle$	A_n^D	Comments
-1	$n^{-2} \langle \epsilon_1^2 \rangle$	$n^0 \langle Z_1^2 \rangle$	$(A_1^D)^{n^2}$	Sharp profile modified by thermal-like scaling factor
$-\frac{1}{2}$	$ n ^{-1} \langle \epsilon_1^2 \rangle$	$ n ^{-1} \langle Z_1^2 \rangle$	$(A_1^D)^{ n }$	Cauchy-like profile
0	$n^0 \langle \epsilon_1^2 \rangle$	$n^2 \langle Z_1^2 \rangle$	$(A_1^D)^{n^2}$	Gaussian profile

particle-size coefficients reduces to the well-known particle function in diffraction theory.

If one takes $r = 0$, each column of cells undergoes either uniform positive or negative strain with $\epsilon_n = \epsilon_1$ for each pair of cells. This type of long-range strain could exist if a distribution of column strain occurs due to fluctuation in the density of embedded atoms. In this case, the Fourier coefficients are assumed to be also of a Gaussian form giving

$$A_n^D = \exp(-2\pi^2 \langle Z_1^2 \rangle n^2 l^2) \quad (2a)$$

which can be obtained from the Fourier transform of a Gaussian profile.

The entry in Table II with $r = -\frac{1}{2}$ reduces to the form treated by Mering.¹⁰ Here the Fourier coefficients are given by

$$A_n^D = \exp(-2\pi^2 \langle Z_1^2 \rangle l^2 |n|), \quad (2b)$$

where $A_1^D = \exp(-2\pi^2 \langle Z_1^2 \rangle l^2)$. Coefficients of the form given in Eq. (2b) are readily summed to give a Cauchy-like profile having a slowly decreasing tail that may not completely go to zero.

Since cold-worked samples average to about $r = -0.46$, one would expect the pure strain profile due to nonuniform strains to be very close to a Cauchy shape. However, additional reshaping will result from small particle size and instrumental broadening.

Particle size

The particle-size Fourier coefficient is given by

$$A_n^S = \frac{1}{N_3} \int_{j=|n|}^{\infty} (j - |n|) P(j) dj, \quad (6)$$

where N_3 is the average number of unit cells per column and $P(j) dj$ is the fraction of columns having lengths between j and $j + dj$ cells. Equation (6) makes use of a continuous representation of the column-length distribution in terms of the integral giving the total number of n th neighbors contributing to a reflection. The line-shape analysis provides only N_3 or $N_3 \langle d \rangle = \langle L \rangle$ and no more particle-size information since the data are not sufficiently accurate to obtain the distribution $p(j)$.

Quantitative microscopy studies provide the line inter-

cepts directly from a lineal analysis of the grains. This can be related to the column-length distribution which is contained in the x-ray Fourier coefficient. The actual distribution of lengths depends upon the grain shape and distribution. Length distributions have already been related to simple shapes,¹³ i.e., to plates and spheres. One distinction should be made between microscopy and x-ray diffraction at this point. In microscopy, only the distribution of grains are under examination; however, in the present problem the coherent size is of importance and this is limited by both subboundaries and grain boundaries. The x-ray particle size is also sometimes taken as an average spacing between dislocations.¹ It will be assumed that the average subgrain shape is related to the overall statistical distribution of dislocations and is spherical. With this assumption, the distribution of lengths intercepted by spheres is given by

$$P(j) = \left(\int_j^{\infty} P(D) dD \right) \left(\int_0^{\infty} j \int_0^{\infty} P(D) dD dj \right)^{-1} \quad (7)$$

with the fraction of sphere diameters between D and $D + dD$ given by $P(D) dD$. In this case, D is expressed in units of $\langle d \rangle$. To minimize the total number of parameters, only a single sphere of average diameter will be considered such that $P(\langle D \rangle) = 1$ and $P(D) = 0$ for $D \neq \langle D \rangle$. For a single sphere the distribution of column lengths is given by

$$P(j) = 8j/9N_3^2 \quad \text{for } j \leq \frac{3}{2}N_3, \quad (8a)$$

and

$$P(j) = 0 \quad \text{for } j > \frac{3}{2}N_3. \quad (8b)$$

This linear distribution is illustrated together with a possible experimental distribution¹⁴ having the same average N_3 in Fig. 2. Introducing Eqs. (8a) and (8b) into Eq. (6) gives the following equations:

$$A_n^S = 1 - \frac{|n|}{N_3} + \frac{4}{27} \left(\frac{|n|}{N_3} \right)^3 \quad \text{for } |n| < \frac{3}{2}N_3, \quad (9a)$$

$$A_n^S = 0 \quad \text{for } |n| \geq \frac{3}{2}N_3. \quad (9b)$$

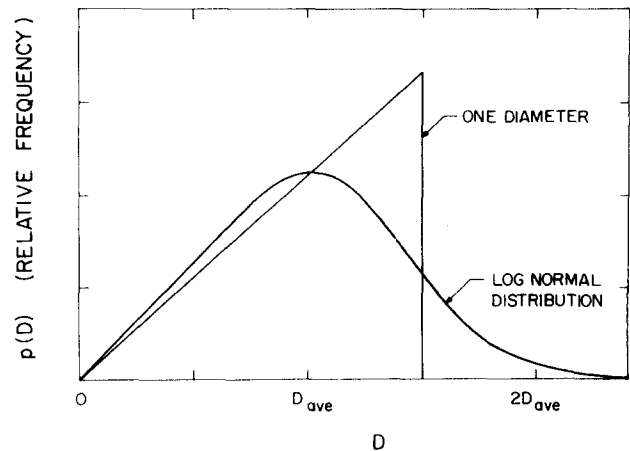


FIG. 2. Column-length distribution from spheres of one size and spheres with a log-normal distribution of diameters.

The first two terms would result from columns of a single height N_3 , while the cubic term allows for the distribution of columns associated with a sphere. From the relation¹

$$\frac{d^2 A_n^S}{dn^2} = \frac{1}{N_3} P(|n|) \quad (10)$$

one can obtain the original distribution of column heights by differentiating only the cubic term.

Instrumental broadening

The instrumental broadening may be included by taking the product of particle-size and strain coefficients and multiplying this by the instrumental broadening coefficients, A_n^I . If a high-resolution diffractometer is used with a monochromator capable of eliminating the K_α component of the K_α doublet, this correction can be included by introducing only one additional parameter. The form of the instrumental broadening curve has been found to be Cauchy-like¹⁵ (see instrumental curve in Fig. 3). Under these conditions, a Cauchy function can be fitted to an annealed sample giving only instrumental broadening. The Fourier series representation of the Cauchy function is

$$f^I(h_3) = \sum_n (A^I)^{|n|} \cos[2\pi n(h_3 - l)] \quad (11a)$$

or in terms of the more usual normalized analytical form

$$\left(\frac{1}{\pi a}\right) \left(1 + \frac{(h_3 - l)^2}{a^2}\right)^{-1} \quad (11b)$$

The Fourier coefficient is related to a by

$$A^I = \exp(-2\pi a), \quad (12)$$

where a can be determined from the semi-half-width according to $h_3^0 - l = a$ and $h_3^0 - l$ is the deviation in reciprocal space that causes the Cauchy to be reduced to one-half its maximum. If the instrumental function is fitted by two half Cauchy functions with the parameters a , and a , then $a = \frac{1}{2}(a_+ + a_-)$. A small shift will also be present [$\phi |n| = -\tanh(2\pi\Delta a |n|)$, with $\Delta a = \frac{1}{2}(a_+ - a_-)$] which can be neglected for a high-resolution diffractometer.

Introducing particle size, strain, and the Cauchy instrumental coefficient into Eq. (1) gives

$$P'(2\theta) = \frac{KNF^2}{\sin^2\theta} \left(1 + 2 \sum_{n=1}^{(3/2)N_3} (A^I)^n A_n^S (A_1^D)^{n^q} \times \cos[2\pi n(h_3 - l)]\right), \quad (1a)$$

where $q = 2(r + 1)$.

Line profile for a film

The authors found that a single Gaussian strain distribution does not adequately describe the state of strain in sputtered Mo films. A least-squares fit of an as-prepared Mo film as well as two others gave $r \cong -\frac{1}{4}$ which is intermediate between the cold-worked value of $-\frac{1}{2}$ and zero for the uni-

form strain. Consequently $r = -\frac{1}{4}$ does not relate directly to a known strain distribution. An equally good fit can be obtained by modifying Eq. (1a) to include two strain distributions. One distribution is associated with pure cold-work strain ($r = -\frac{1}{2}$), while the other describes variations in the uniform column strain ($r = 0$). The combined distribution of strain is given by the following integral:

$$P_R(Z_n) = \int_{-\infty}^{\infty} P_D(Z'_n) P_U(Z_n - Z'_n) dZ'_n \quad (13)$$

The integral can generally be taken to infinite limits because of the rapid convergence of the distribution functions over the region $\pm \frac{1}{2}\langle d \rangle$. If one assumes the distribution of uniform column strain to be Gaussian about the average, the introduction of dislocations from cold working causes an additional smearing of the strain distribution and an r value between $-\frac{1}{2}$ and 0. Variations in the uniform column strain could occur as a result of statistical variations of embedded ions during the sputtering process.

The Gaussian distribution $P_R(Z_n)$ which results from the convolution of two pure Gaussian distributions allows a simple calculation of the resultant Fourier coefficient. By using this function

$$P_R(Z_n) = P_0 \exp\left(-\frac{1}{2} \frac{Z_n^2}{n^2(\langle Z_{1D}^2 \rangle/n + \langle Z_{1U}^2 \rangle)}\right) \quad (14)$$

and

$$\begin{aligned} \langle \cos 2\pi l Z_n \rangle &= \int_{-\infty}^{\infty} P_R(Z_n) \cos(2\pi l Z_n) dZ_n \\ &= \exp\left[-2\pi \left(\frac{\langle \epsilon_{1D}^2 \rangle}{n} + \langle \epsilon_{1U}^2 \rangle\right) n^2 l^2\right], \quad (15) \end{aligned}$$

where P_0 is a normalization factor, ϵ_{1D} and ϵ_{1U} are first neighbor nonuniform strains arising from cold working and variations in the uniform column strain, respectively. Equation (15) can be written equally in terms of strain or displacement since $\epsilon_1 = Z_n/n$. The sum of exponential terms very conveniently reduces the strain Fourier coefficient to an equivalent product of coefficients

$$A_{1F}^D = (A_1^U)^{n^q} (A_1^D)^{|n|}$$

with

$$A_1^U = \exp(-2\pi^2 \langle \epsilon_{1U}^2 \rangle l^2)$$

and

$$A_1^D = \exp(-2\pi^2 \langle \epsilon_{1D}^2 \rangle l^2).$$

This definition of A_1^D is physically more realistic in studies of deformed films and does not require an interpretation of r values other than $-\frac{1}{2}$ and 0.

The quantities $\langle \epsilon_{1U}^2 \rangle^{1/2}$ and $\langle \epsilon_{1D}^2 \rangle^{1/2}$ are defined as first neighbor strains. This interpretation should be made only with considerable caution since accurate measurements of strain from peak profiles are reported only over a range from about ten cell heights to about N_3 . It is likely that the tail portions of the various profiles are so slowly varying that

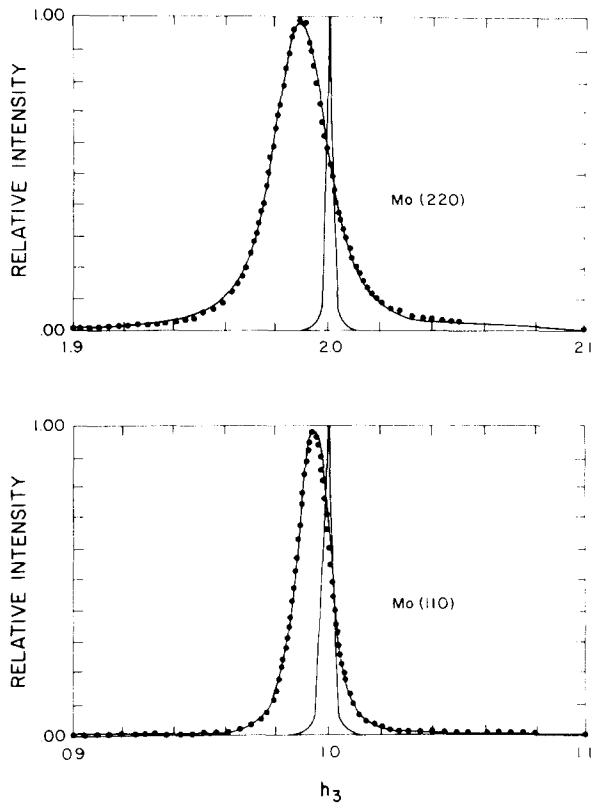


FIG. 3. Least-squares fit of 110 and 220 profiles obtained from a 1.5- μm Mo film on a (111)-oriented single crystal. The points represent the experimental curve with instrumental broadening. The sharp Cauchy-like instrumental functions from annealed Mo powder with Cu K_{α} radiation are also illustrated.

diffuse scattering measurements would be required to obtain a sufficiently accurate representation for near-neighbor strains. Most often this would be obscured by overlapping profiles. Consequently, the first neighbor rms strains are characteristic of intermediate distances up to the average particle size and are valid for extrapolating the strain over this range. These parameters should be of value for inter-comparing the state of nonuniform strain between different films under a range of conditions provided these limitations are kept in mind.

APPLICATION OF SIMPLIFIED THEORY

Data were collected from a 1.5- μm deposit of Mo on a 111-oriented Si crystal. The 110 and 220 provided a pair of reflections which allow particle size and strain coefficients to be separated.¹ The K_{α} component of the K_{α} doublet was eliminated using a Jogodzinski high-resolution quartz incident beam monochromator, a fine focus x-ray tube, and 0.05-mm receiver slit. A well-annealed power of Mo was used to determine the Cauchy coefficient A^l according to Eq. (12).

A linear background correction could be made for the (110) peak; however, this was not possible for the (220). The (220) is located on the tail portion of the strong Si (333) reflection, making the background somewhat nonlinear. It

was found that a suitable correction could be made by fitting the overlap region with a Pearson VII function.¹⁶ In fitting Eq. (1a) to the experimental peaks [Figs. 1(a) and 1(b)], a nonlinear least-squares curve-fitting program was used. The quantities N_3 , $\langle \epsilon_1^2 \rangle$, q , $\langle d \rangle$, and the peak height were varied in the computer analysis with the fits illustrated in Fig. 3. The computer program used is a modified version of IBM SHARE program No. 3094. In order to verify that the curve-fitting program converges under typical conditions, Eq. (1a) was synthesized with $r = 0.5$ and a range of A_1^D as well as N_3 values were used. In all cases, the program converged to the exact parameters originally used to synthesize the Fourier series.

The computer program gave the following results for a sputtered Mo film having an average substrate temperature of 350 °C: $\langle L \rangle = N_3 \langle d \rangle = 215 \text{ \AA}$, $\langle \epsilon_1^2 \rangle^{1/2} = 0.012$, and $r = -0.27$. This can be compared with results obtained from Mo filings and the same set of (110) planes. These were reported as $\langle L \rangle = 260 \text{ \AA}$, $\langle \epsilon_1^2 \rangle^{1/2} = 0.0201$, and $r = -0.56$. A comparison between the two data sets indicates that the average particle size is close but a little smaller in the Mo film. Also, $\langle \epsilon_1^2 \rangle^{1/2}$ and r are about twice as large for the cold-worked powder. The smaller r value which is characteristic of the film causes the strain to fall off more slowly. Even though the first neighbor strain is smaller for the film, the long-range nonuniform strain is greater in the film because of the smaller value of r . The variation in these quantities with annealing time is discussed in greater detail elsewhere.¹⁷

ACKNOWLEDGMENT

Funding for this study was made available by National Science Foundation Grant No. DMR-17201.

APPENDIX

The strain Fourier coefficient in the most general form is given by $\langle \exp(-2\pi i Z_n l) \rangle$. Mering¹⁰ has assumed for spacing disorder problems that the individual first neighbor displacements are independent. If one selects the m th cell of a column as an origin, the displacement of the n th neighbor is given by the sum individual terms

$$Z_{m,n} = Z_{m+1} + Z_{m+2} + \dots + Z_{m+n}. \quad (\text{A1})$$

Substituting into the Fourier coefficient and averaging over all n th neighbors in the sample

$$\begin{aligned} \langle \exp(-2\pi i Z_n l) \rangle_m &= \langle \exp(-2\pi i Z_{m+1} l) \rangle \langle \exp(-2\pi i Z_{m+2} l) \rangle \dots \\ &\times \langle \exp(-2\pi i Z_{m+n} l) \rangle. \end{aligned} \quad (\text{A2})$$

If each term of the product is independent, then each is the same because they are determined by the same unspecified first neighbor distribution function. This gives

$$\langle \exp(-2\pi i Z_n l) \rangle = \langle \exp(-2\pi i Z_1 l) \rangle^{n!} \quad (\text{A3})$$

and by expanding the first neighbor coefficient assuming $2\pi i Z_1 l \ll 1$ gives

$$\langle \exp(-2\pi i Z_1 l) \rangle = 1 - \frac{1}{2} \langle 2\pi i Z_1 l \rangle^2 + (1/4!) \langle 2\pi i Z_1 l \rangle^4. \quad (\text{A4})$$

The odd terms are normally dropped because of symmetry about the origin at each distance $\langle d \rangle n$. If terms higher than the second can be ignored

$$\langle \exp(-2\pi i Z_1 l) \rangle = \exp(-2\pi^2 \langle \epsilon_1^2 \rangle l^2) = A_1^D. \quad (\text{A5})$$

The Fourier series representing strain broadening is given by

$$\sum_{n=-\infty}^{\infty} (A_1^D)^{|n|} \cos[2\pi n(h_3 - l)] \quad (\text{A6})$$

which can be summed to give a Cauchy-like function.

The expanded form of the coefficient as given in Eq. (A5) is valid for the first two orders of a strain-particle-size analysis even for the largest values of $\langle \epsilon_1^2 \rangle$ given in Table I. In this development, $r = -\frac{1}{2}$ (see Table II). However, this is a consequence of the independence between first neighbor displacements rather than the variation of the displacements with distance. It is not likely that the average value of $r = -0.46$ found with cold-worked samples is due to independent displacements. Instead, it should be due to correlated atomic displacements resulting from the strain fields of dislocations.

¹B.E. Warren, *Prog. Metal Phys.* **8**, 147 (1959).

²C.N.J. Wagner, *Local Atomic Arrangements Studied by X-Ray Diffraction*, edited by J.B. Cohen and J.E. Hilliard (Gordon and Breach, New York, 1966).

³R.L. Rothman and J.B. Cohen, *Advances in X-Ray Analysis Vol. 12*, edited by C.S. Barrett, J.B. Newkirk, and G.R. Mallett (Plenum, New York, 1969).

⁴B.D. Cullity, *Elements of X-Ray Diffraction* (Addison-Wesley, Reading, Mass., 1978).

⁵M. McKeehan and B.E. Warren, *J. Appl. Phys.* **24**, 52 (1953).

⁶B.E. Warren and E.P. Warekois, *Acta Metall.* **3**, 473 (1955).

⁷J. Despujols and B.E. Warren, *J. Appl. Phys.* **29**, 195 (1958).

⁸E.N. Aqua and C.N.J. Wagner, *Philos. Mag.* **9**, 565 (1964).

⁹W.P. Evans, R.E. Ricklefs, and J.F. Millan, in Ref. 2.

¹⁰J. Mering, *Acta Crystallogr.* **2**, 371 (1949).

¹¹J.W. Harrison, *Acta Crystallogr.* **20**, 390 (1966).

¹²R.J. DeAngelis, in Ref. 2.

¹³J.W. Cahn and R.L. Fullman, *Trans. AIME* **206**, 610 (1956).

¹⁴S.A. Saltykov, *Stereometric Metallography*, 2nd ed. (Armed Service Technical Info. Moscow, 1958).

¹⁵E.R. Pike, *Acta Crystallogr.* **12**, 87 (1959).

¹⁶M.M. Hall, V.G. Veeraraghavan, R. Herman, and P.G. Winchell, *J. Appl. Crystallogr.* **10**, 66 (1977).

¹⁷T. Adler and C.R. Houska, following paper, *J. Appl. Phys.* **50**, 3288 (1979).